Nonequilibrium Radiative Heating of an Ablating Jovian Entry Probe

S. N. Tiwari* and S. V. Subramanian†
Old Dominion University, Norfolk, Virginia

The influence of nonlocal thermodynamic equilibrium (NLTE) radiative transfer on the entire range of shock-layer flow phenomena around a Jovian entry body is investigated. The entry body considered is a 35 deg hyperboloid. The flow in the shock layer is assumed to be viscous, axisymmetric, laminar, and in chemical equilibrium. With coupled ablation carbon-phenolic injection, 16 chemical species are used in the ablation layer for radiation absorption. The NLTE radiative transfer and flux equations are expressed in terms of the NLTE source function, collisional relaxation time, and radiative lifetime. The NLTE results obtained for the peak-heating entry conditions are compared with corresponding equilibrium results. The results indicate that, in the presence of the ablative products, the radiative heating to the entry body is significantly higher under NLTE conditions.

Nomenclature

A_{nm} = Einstein coefficient for spontaneous emission
$A'\pi_u$ = lower electronic energy level for the C_2-Freymark transition
$a^3\pi_u$ = lower electronic energy level for the C_2-Swan transition
B_{nm} = Einstein coefficient for stimulated emission
B_ν = Planck's function
C_{nm} = collisional de-excitation rate coefficient
c = speed of light
$D'\Sigma_u^+$ = upper electronic energy level for the C_2-Mulliken transition
$d^3\pi_g$ = upper energy level for the C_2-Swan transition
$E'\Sigma_g^+$ = upper energy level for the C_2-Freymark transition
$F_{v'v''}$ = band oscillator strength
h = Planck's constant
I_ν = intensity of radiation
$I_{\Delta\nu}$ = mean radiation intensity averaged over the spectral interval $\Delta\nu$
J_ν = source function
k = Boltzmann constant
N_m = number density of the particles in the mth level
N_n = number density of the particles in the nth level
n = coordinate normal to the body surface, n^*/R_N^*
q_R = net radiative heat flux
$q_{R\nu}$ = spectral radiative heat flux
R_N = body nose radium, cm
R_b = base radius, cm
s = coordinates along the body surface, s^*/R_N^*
T = equilibrium temperature, K
V_∞ = freestream velocity, km s^{-1}
$x'\Sigma_g^+$ = lower energy level for the C_2-Mulliken transition
η = NLTE parameter, η_c/η_r
η_c = collisional relaxation time, s
η_r = radiative lifetime of the excited state, s
κ_ν = spectral absorption coefficient, cm^{-1}
$\bar{\kappa}_\nu$ = equilibrium spectral absorption coefficient, cm^{-1}
ρ = density of shock-layer gas, kg m^{-3}
τ = optical coordinate

Subscripts

∞ = freestream values
$m,0$ = lower energy level
$n,1$ = upper energy level
s = values at shock
w = values at wall

Superscripts

$(\,)''$ = lower state of the energy level
$(\,)'$ = upper state of the energy level
$(\,)^*$ = dimensional quantity

I. Introduction

In order to study the composition and structure of Jupiter's atmosphere, NASA has planned a Galileo mission for the near future. The Galileo probe is expected to enter Jupiter's atmosphere with an array of scientific instruments. At Jovian entry conditions, the heating is so severe that the probe has to be protected by heat-shield materials that weigh as much as 50% of the total probe weight.[1-3] The probe's heating is primarily due to radiation from the high-temperature shock-layer gases. Since the experimental facilities are not capable of a full simulation of the exact nature of all of the important thermal phenomena speculated during Jovian entry, it is necessary to rely on the analytical studies for the design of the entry probe. In order to evaluate the magnitude of the radiative heating of the entry body, a meaningful radiative transport model has to be employed. In the analytical expression of the transfer equation for the radiating gases, it is normally assumed that the gas is in the local thermodynamic equilibrium (LTE). There are situations, however, where this assumption may not be justified and the condition of nonlocal thermodynamic equilibrium (NLTE) may prevail.

The LTE analytical studies of the aerothermal environment for the Jupiter probe have shown that, for a phenolic-carbon heat shield under laminar flow conditions, nearly 50% of the radiation emitted in the high-temperature shock-layer region of the flowfield is absorbed within the cooler ablation layer adjacent to the body surface.[4-6] The radiation absorption is primarily due to the absorption of the C_2 and C_3 molecules.[7-9] It is, therefore, important to investigate the effects of NLTE on the entire range of shock-layer flow phenomena in the presence of the ablative products.

Only a few NLTE analyses dealing with planetary entry heating are available in the literature.[10-12] Horton[10] and

Presented as Paper 80-0356 at the AIAA 18th Aerospace Sciences Meeting, Pasadena, Calif., Jan. 14-16, 1980; submitted May 12, 1982; revision received Jan. 3, 1983.

*Eminent Professor, Dept. of Mechanical Engineering and Mechanics. Member AIAA.

†Graduate Research Assistant; presently, Development Engineer, Avco-Lycoming, Stratford, Conn. Member AIAA.

Tiwari and Subramanian[11] investigated the influence of NLTE on the entry heating in absence of ablative products. For Jovian entry conditions, results obtained in Ref. 11 indicate that the NLTE radiation, in general, reduces the radiative heating to the entry body in the absence of the ablative products. Recently, Nelson[12] presented the parametric equations for nonequilibrium radiative transport in the stagnation ablation layer. However, no specific results were obtained to investigate the effects of NLTE on the aerothermal environment of the entry body for critical entry conditions.

The purpose of this study is to formulate the NLTE governing equations under physically realistic conditions for Jovian entry in presence of the ablative products, investigate all of the shock-layer flow phenomena, and determine the extent of NLTE heating rates for critical (peak-heating) entry conditions. It should be pointed out that this study deals only with the influence of NLTE radiative transfer on the shock-layer flow phenomena in the presence of the ablative products; the shock-layer species, however, are assumed to be in chemical equilibrium.

II. Basic Formulation

The physical model and coordinate system for a Jovian entry body (probe) are shown in Fig. 1. The radiating flow in the shock layer is assumed to be axisymmetric, steady, viscous, and in chemical equilibrium. Basic governing equations for this physical model (with coupled mass injection and ablation) are available in Refs. 5 and 13-15. Thus, only the governing equations for NLTE radiative transfer and radiative flux are presented in this section.

The equation of radiative transfer may be expressed, in general, as[15,16]

$$dI_\nu/dn=\rho\kappa_\nu(J_\nu-I_\nu) \tag{1}$$

where

$$\kappa_\nu=\bar{\kappa}_\nu[1-(N_n/N_m)(B_{nm}/B_{mn})] \tag{2}$$

$$J_\nu=A_{nm}/\{B_{nm}[(N_m/N_n)(B_{mn}/B_{nm})-1]\} \tag{3}$$

$$A_{nm}=(2h\nu^3/c^2)B_{nm}, \qquad B_{nm}=(g_m/g_n)B_{mn} \tag{4}$$

In the above equations, N_m and N_n represent the number densities and g_m and g_n the statistical weight factors for the lower and upper energy levels, respectively. For nonequilibrium conditions, the state population ratio (N_m/N_n) for any two levels in a multilevel system consisting of k levels is expressed as[17]

$$N_m/N_n=\sum_k P_{nk}Q_{km,n}\Big/\sum_k P_{mk}Q_{kn,m} \tag{5}$$

where P_{nk} is the sum of the radiative term A_{nk} and the collision term C_{nk}. The quantity $Q_{km,n}$ is the probability for all transitions from level k to m not involving n, such that for $k=m, Q_{kk,n}=1$.

Upon combining Eqs. (3-5), the source function for the transition between levels n and m (containing k intermediate levels) is given by[11,15,18]

$$J_\nu=\left[\int_{\Delta\nu} I_\nu^*\phi_\nu d\nu+\epsilon^*+\theta^*\right]\Big/(1+\epsilon^*+\eta^*-\delta\theta) \tag{6}$$

where

$$\theta=\frac{1}{B_{mn}}\sum_{\substack{\ell=1\\ \ell\neq n,m}}^{k} P_{m\ell}Q_{\ell n,m} \tag{7a}$$

$$\eta^*=\frac{1}{A_{nm}}\sum_{\substack{\ell=1\\ \ell\neq n,m}}^{k} P_{n\ell}Q_{\ell m,n} \tag{7b}$$

$$\epsilon^*=C_{nm}/[B_{mn}B_\nu(T)] \tag{7c}$$

$$\delta=c^2/2h\nu^3, \qquad I_\nu^*=I_\nu/B_\nu(T), \qquad \theta^*=\theta/B_\nu(T) \tag{7d}$$

For a three-level transition, Eq. (6) reduces to[11]

$$J_\nu=\{(2h\nu^3/c^2)/[\exp(h\nu/kT)-1]\}\times[1+\eta(\bar{I}_{\Delta\nu}/\bar{B}_{\Delta\nu})+\delta_1]/(1+\eta+\delta_2) \tag{8}$$

where

$$\bar{B}_{\Delta\nu}=4\pi\int_{\Delta\nu} B_\nu d\nu \tag{9a}$$

$$\delta_1=C_{02}(A_{21}+C_{21}+B_{21}\bar{I}_{\Delta\nu})/(B_{01}Q_T) \tag{9b}$$

$$\delta_2=[C_{20}(B_{12}\bar{I}_{\Delta\nu}+C_{12})-C_{02}(A_{21}+C_{21}+B_{21}\bar{I}_{\Delta\nu})]/(A_{10}Q_T) \tag{9c}$$

$$Q_T=A_{21}+B_{21}\bar{I}_{\Delta\nu}+C_{21}+C_{20} \tag{9d}$$

In the preceding equations, $\eta=A_{10}/C_{10}$ represents the ratio of the collisional deactivation (or relaxation) time and radiative lifetime of the first excited state, and quantities δ_1 and δ_2 are the influence factors in the NLTE source functions arising from the higher level energy transitions. For a two-level transition the expression for the source function, as given by Eq. (8), further simplifies as[19]

$$J_\nu=B_\nu-\left\{\eta\left[\int_{\Delta\nu}\frac{dq_R}{dy}d\nu\right]\Big/4\pi\int_{\Delta\nu}\kappa_\nu d\nu\right\} \tag{10}$$

It is evident from Eqs. (8-10) that the degree of NLTE depends on the magnitude of quantities η, δ_1, and δ_2. Since values of δ_1 and δ_2 are always lower than η for all particles involving multilevel energy transitions, the extent of nonequilibrium is characterized essentially by the parameter η. By theoretical considerations, Jefferies[17] has established that the value of $\delta_{1,2}/\eta$ is approximately 0.1 for most gases involving multilevel energy transitions. Consequently, for $\eta\ll 1$, the source function becomes the Planck function, and the assumption of LTE is justified. On the other hand, the condition of radiative equilibrium is reached for $\eta\gg 1$, and in this case the entire process of excitation and de-excitation is radiatively controlled. The NLTE radiation becomes important for conditions where $\eta=0(1)$. Equation (8) is used in evaluating the nonequilibrium source function when no ablation mass injection is considered in this study. With ablation injection in the shock layer, Eq. (10) is used for the evaluation of J_ν to simplify the analysis.

For a two-level transition, the expression for the nonequilibrium absorption coefficient can be obtained from Eq. (2) as[15]

$$\kappa_\nu=\bar{\kappa}_\nu(0,1)\left\{1-\left[\eta+\frac{\eta}{\delta}\int_{\Delta\nu} q_{R\nu}d\nu\right]\Big/\mathrm{DEN}\right\} \tag{11}$$

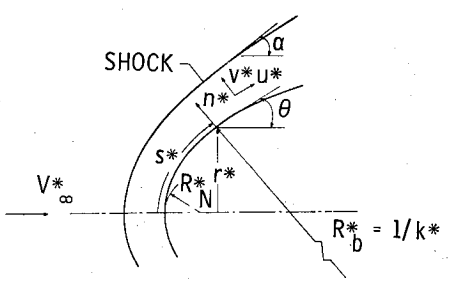

Fig. 1 Physical model and coordinate system.

where

$$\bar{\kappa}_\nu(0,1) = \sigma_\nu(0,1) N_0 \tag{12a}$$

$$\text{DEN} = (\eta/\delta) + \exp(-h\nu/kT) \tag{12b}$$

In Eq. (12a), $\sigma_\nu(0,1)$ represents the absorption cross section and N_0 is the number density of the absorbing species in the ground state.

The "tangent slab" assumption for radiative transport is used in this study. With this assumption, the expression for the NLTE radiative flux is obtained by integrating the NLTE transfer equation, Eq. (1), between two parallel boundaries (the body and the shock) as[14,15]

$$q_R(n) = q_R^+(n) - q_R^-(n) = \int_0^\infty q_{R\nu}^+(\tau_\nu)\,d\nu - \int_0^\infty q_{R\nu}^-(\tau_\nu)\,d\nu \tag{13}$$

where

$$q_R^+(n) = 2\int_0^\infty \left[B_{I\nu}E_3(\tau_\nu) + \pi\int_0^{\tau_\nu} J_\nu(t)E_2(\tau_\nu - t)\,dt\right]d\nu \tag{14a}$$

$$q_R^-(n) = 2\int_0^\infty \left[B_{2\nu}E_3(\tau_{0\nu} - \tau_\nu) + \pi\int_{\tau_\nu}^{\tau_{0\nu}} J_\nu(t)E_2(t - \tau_\nu)\,dt\right]d\nu \tag{14b}$$

$$\tau_\nu = \int_0^n \kappa_\nu(n)\,dn \tag{14c}$$

In Eq. (13), q_R^+ and q_R^- represent the radiative flux toward the shock and body, respectively. In Eqs. (14), $B_{I\nu}$ and $B_{2\nu}$ represent the radiosities of the body and shock, respectively; and expressions for these are available in the cited references.

With appropriate relations for κ_ν and J_ν, Eq. (13) is used in the general energy equation and the set of governing equations is solved for desired results.

III. Properties of the Shock-Layer Gas

For Jovian entry conditions and for the case with no ablation from the surface, the NLTE effects are considered only for the hydrogen species in the shock layer. However, for the case of carbon-phenolic (or graphite) ablation injection, the C_2 molecules play a very important role in the radiation blockage. For this case, therefore, contributions for the C_2 molecules are included in the NLTE analysis.

Complete information on chemical composition and thermodynamic and transport properties of the shock-layer gas (with and without ablative products) is available in Refs. 5 and 13-15. Information on radiative and collisional properties for different species is obtained from various sources. This is discussed briefly in this section.

A. Absorption by Gaseous Mixture

The equilibrium absorption coefficient, in the spectral range 0-15 eV, is evaluated by using the detailed method described in Refs. 15 and 20. Appropriate modifications are made in this model to account for NLTE processes.[11,15] In particular, the absorption coefficient for the C_2 molecules which includes all the important band systems in the spectral range of 0.1-6.6 eV is evaluated using the method outlined in Ref. 8.

It should be noted that for evaluation of the NLTE absorption coefficient and source function, it is essential to have information on the collisional relaxation time and radiative lifetime of different species. This information is available for the shock-layer species without ablative products in Refs. 11 and 15; and the method of evaluating this in presence of the ablative products is presented in the next two subsections.

B. Collisional Relaxation Time

The important species influencing the collisional process in the ablative layer are C_2, H_2, H, H^+, C_3, C, and e^-. The effect of molecular hydrogen, however, is negligible because the number density of H_2 is small compared to the other species. Experimental values for the collisional relaxation time for C_2 are not available in the literature. However, these can be obtained from theoretical considerations similar to that for shock-layer species without ablation injection.[11,15]

The collisional relaxation time for collisions between neutral particles (such as atoms and molecules) is given, in general, by[15,21]

$$\eta_c = 1/f_c = 1/(\Omega n v) = (\pi m/8kt)^{1/2}/(\Omega n) \tag{15}$$

where f_c is the frequency of collisions (s^{-1}), n the number density of the colliding particles (cm^{-3}), Ω the collisional cross section of the colliding particles (cm^2), v the most probable velocity of the particles (cm-s^{-1}), and m the mass of the colliding particles. The relaxation time for collisions between like particles (i.e., for H-H, H_2-H_2, C_2-C_2 collisions) can be obtained from Eq. (15) by using appropriate values for collisional cross section and mass. For C_2, $\Omega = 2.5\times10^{-8}$ and $m = 4\times10^{-23}$ g. For collisions between unlike particles (with different mass and cross section), the relaxation time is given by[15,21]

$$n_c^{-1}(\text{C-C}_2) = 2n_{C_2}\Omega_E[2kT(m_{C_2} + m_C)/(\pi m_{C_2} m_C)]^{1/2} \tag{16}$$

where

$$\Omega_E = 0.25(\Omega_{C_2} + \Omega_C) + (\tfrac{1}{2}\pi)(\Omega_{C_2}\Omega_C)^{1/2} \tag{17}$$

The combined relaxation time for self-collisions and collisions of different kind is given by[15]

$$1/[\eta_c(\text{COM})] = X/[\eta_c(\text{C-C})] + (1-X)/[\eta_c(\text{C}_2\text{-C})] \tag{18}$$

where X represents the mole fraction of C.

The rate of electronic de-excitation from an upper state to a lower state (by electron impact in a molecule) is given by[21]

$$C_{nm} = [A(T/10{,}000)^r g_k]/(\bar{m}^5/\bar{n}^5)\,[(1/\bar{m}^2) - (1/\bar{n}^2)] \tag{19}$$

where g_k is the statistical weight factor, $\bar{m}$ and $\bar{n}$ are the principal quantum numbers of the lower and upper states, respectively, A is the excitation rate constant (different for different molecules), and r represents the internuclear separation distance the value of which is different for different molecules. Due to the absence of e^- close to the wall, where the NLTE effect is more pronounced, de-excitation by electronic collisions is not considered.

C. Radiative Lifetime of Excited States

There are eight known C_2-band systems in the 0.2 to 7.0 eV (0.1 to 1.2 μ) spectral region. The Swan band system, whose electronic transition is represented by $d^3\pi_g - a^3\pi_u$ is the strongest radiating system of the C_2 molecules. The Freymark band ($E'\Sigma_g^+ - A'\pi_u$) and the Mulliken band ($D'\Sigma_u^+ - x'\Sigma_g^+$) are the next important radiating systems of the C_2 molecules. Hence, the radiative lifetime of these band systems has to be determined first in order to evaluate their respective NLTE cross sections. For a molecule with an electronic transition, the radiative lifetime is related to the wavelength-dependent electronic F number, the electronic transition moment, and the Einstein coefficient for spontaneous emission $A_{n'n''}$. The measured value for the electronic transition moment is available for the C_2-band systems.[22] The electronic F number is given in terms of the square of the transition moment $|R_e/ea_0|^2$ as

$$F_{el}(\lambda) = [(8\pi^2 m_e c/3he^2\lambda)\Sigma|R_e/ea_0|^2]/A \tag{20}$$

where

$$A = (2 - \sigma_{0,\Lambda''})(2S'' + 1)$$

In the above discussions and relations, the single prime denotes the upper state and the double prime the lower state,

and S'' represents the spin quantum number of the lower state. The quantity $\sigma_{0,\Lambda}=1$ for $\Lambda=0$ and $\sigma_{0,\Lambda}=0$ for $\Lambda\neq 0$; Λ is the resultant angular momentum of electrons. The electronic F number is related to the band oscillator strength by

$$F_{v'v''}=F_{el}q_{v'v''} \tag{21}$$

where $q_{v'v''}$ is the Franck-Condon factor. Now, the radiative lifetime of the v'' state can be expressed as

$$(n_r)^{-1}=A_{v'v''}=F_{v'v''}\left[(6.67\times 10^{15})/\lambda^2\right](g''/g') \tag{22}$$

Here, g' and g'' are the degeneracies of the upper and lower levels, respectively, and $g''/g'=1$ if the corresponding vibrational levels of the electronic state are nondegenerate. The value of $F_{v'v''}$ measured for the C_2-Swan (0,0) band is 6.5×10^{-3} (Ref. 23). Upon substituting this value of $F_{v'v''}$ and using Eq. (22), the radiative lifetime of the C_2-Swan $3\pi_g$ $(v'=0)$ state is found to be 8.0×10^{-7} s. No measured value of the band oscillator strength $F_{v'v''}$ is available for the Freymark and Mulliken band system. However the values of the electronic transition moment are available for these bands; and, since $F_{v'v''}$ is directly proportional to the electronic transition moment, the radiative lifetime of the $E'\Sigma_g^+$ state of the Freymark (0,1) band is 1.5×10^{-6} s and the $D'\Sigma_u^+$ of the Mulliken (0,0) band is 6.95×10^{-6} s. These values are used in the majority of cases investigated in the present study. However, another set of values for the radiative lifetime of different bands is suggested in the literature.[22] These are η_r (Swan) $=1.25\times 10^{-7}$ s, η_r (Freymark) $=4.67\times 10^{-8}$ s, and η_r (Mulliken) $=8.77\times 10^{-9}$ s. These values are significantly different from those mentioned earlier. Because of this discrepancy, it is essential to investigate the influence of a different set of radiative lifetimes on the NLTE results. The following format, therefore, will be adapted for calculating the NLTE results in the presence of the ablative products in the shock layer:

NLTE (I): based on η_r (Swan) $=8\times 10^{-7}$ s.

NLTE (II): based on η_r (Swan) $=1.25\times 10^{-7}$ s.

NLTE (III): based on the combined contributions of η_r (Swan) $=8\times 10^{-7}$, η_r (Freymark) $=1.5\times 10^{-6}$, and η_r (Mulliken) $=6.95\times 10^{-6}$ s.

NLTE (IV): based on the combined contributions of η_r (Swan) $=1.25\times 10^{-7}$, η_r (Freymark) $=4.67\times 10^{-8}$, and η_r (Mulliken) $=8.77\times 10^{-9}$ s.

IV. Computational Procedure and Data Source

The numerical procedure for solving the viscous shock-layer equations with coupled injection is discussed in detail in Refs. 5 and 13. The entry body considered is a 35 deg half-angle hyperboloid which enters the Jovian atmosphere at zero angle of attack. The body nose radius is $R_N^*=0.311$ m. The body surface is assumed to be gray having a surface emittance of 0.8. Jupiter's nominal atmosphere is assumed to consist of 89% hydrogen and 11% helium by volume. Complete information on thermodynamic and transport properties, entry trajectory, and other data required for the present study is available in Refs. 5, 13, and 15.

V. Results and Discussion

To investigate the importance of NLTE radiation, the results were obtained only for a 35 deg hyperboloid (with coupled ablation mass loss from a carbon-phenolic heat shield). This is because, for this case, LTE results were already available in the literature.[5-9] For comparative purposes, selected NLTE results were also obtained for the case with no ablative products (i.e., for $\dot{m}=0$). The NLTE results, in this case, were obtained by considering the combined collisional deactivation process of H-H and H^+-H^+. The combined relaxation time is obtained by using the appropriate form of Eq. (18). Viscous shock-layer results obtained for the peak-heating conditions are presented in this section.

As discussed earlier, for NLTE study, it is essential to know the nature of the collisional de-excitation processes and relaxation times of different shock-layer species in the presence of the ablative products. Figure 2 illustrates the important species concentrations near the wall influencing the C_2 collisional process. In general, the C_3 molecules are concentrated near the wall and the number density rapidly reduces away from the wall as they dissociate into C_2 and atomic carbon.

The variation of collisional relaxation time for the C_2-C_2, H-H, and combined collisions is shown in Fig. 3 as a function of temperature. The C_2-C_2, C_2-C, C_2-H, and H-H collisions represent the combined collisional process. This relaxation time for the combined collisional process is used in the present analysis. The radiative lifetimes of the Swan (0,0), Freymark (0,1), and Mulliken (0,0) bands are also shown in this figure. Unlike the collisional relaxation time, the radiative lifetimes is invariant with temperature. The majority of NLTE results in

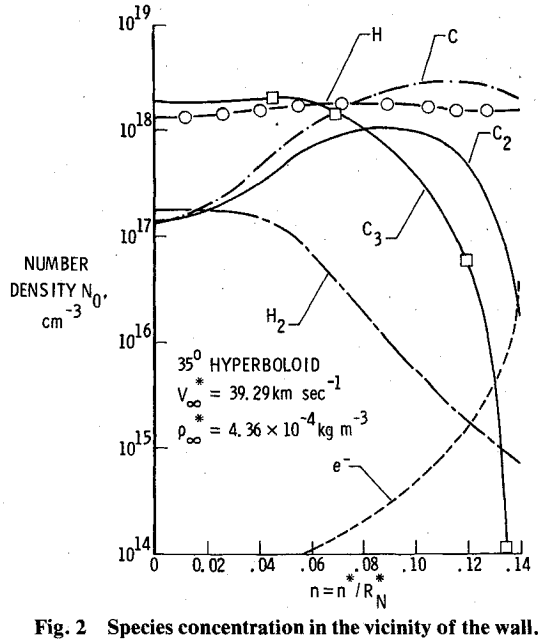

Fig. 2 Species concentration in the vicinity of the wall.

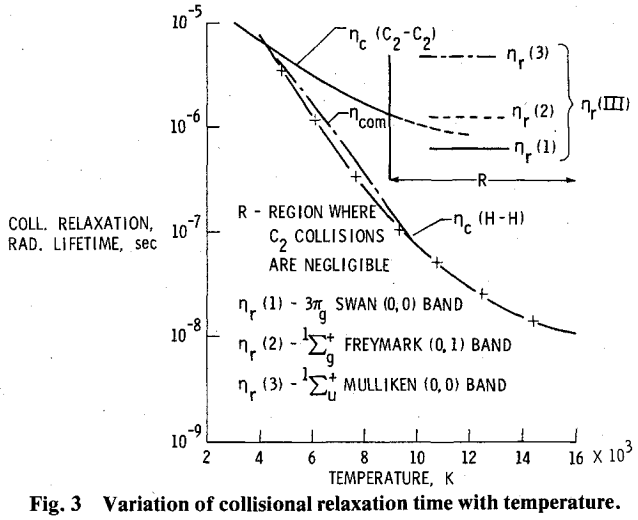

Fig. 3 Variation of collisional relaxation time with temperature.

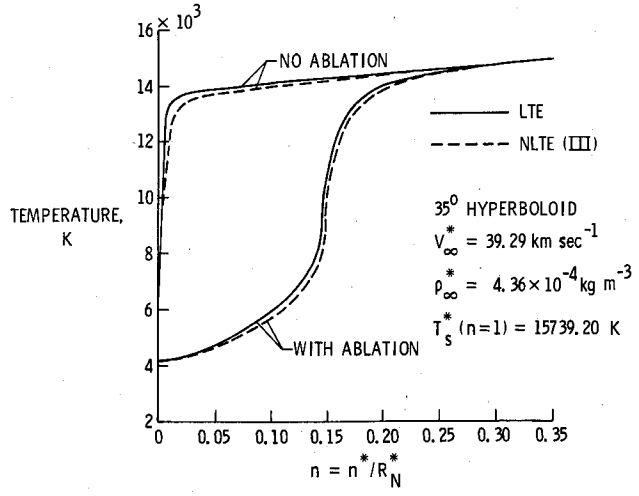

Fig. 4 Temperature distribution across the shock layer (along the stagnation streamline).

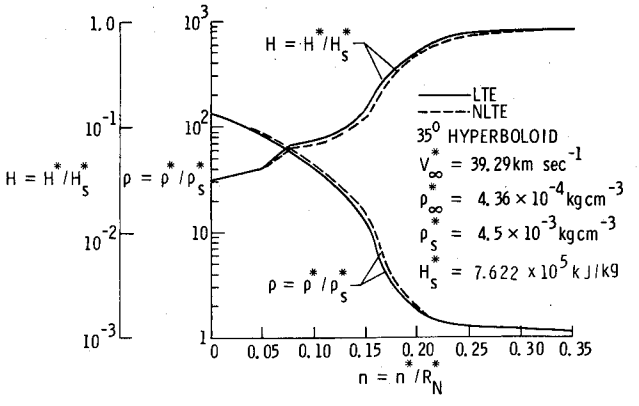

Fig. 5 Enthalpy and density variations across the shock layer (along the stagnation streamline).

this study were obtained by using the combined radiative lifetimes of the Swan, Freymark, and Mulliken band systems as indicated by η_r (III). However, some results for radiative heating rates were also obtained by using the other radiative lifetimes of the band system as indicated by η_r(I), η_r(II), and η_r(IV).

The temperature variation across the shock layer (for location $s=0$) is shown in Fig. 4 for both LTE and NLTE (III) conditions. Results with no mass injection are also shown here for comparison. As would be expected, the shock-layer temperature, in general, is lower in the vicinity of the body in the presence of the ablative products. It is seen that the NLTE temperature distribution is lower than the equilibrium values throughout the shock layer. A maximum difference of 5.48% is noticed between the two values at $n=0.13$. The C_2 molecules in the ablation layer absorb less energy under NLTE conditions than under equilibrium conditions. This, in turn, results in lower temperature values in the ablation layer, and this trend continues in the entire shock layer.

Figure 5 illustrates the density and enthalpy variations across the shock layer for LTE and NLTE (III) conditions. The enthalpy variation has a similar trend as the shock-layer temperature shown in Fig. 4. It was found that NLTE essentially had no influence on the pressure distribution in the shock layer. The density, however, is seen to be significantly higher for the NLTE case. This is a direct consequence of relatively lower NLTE temperatures in the shock layer. A maximum increase in density of about 5.5% is noticed at $n=0.15$.

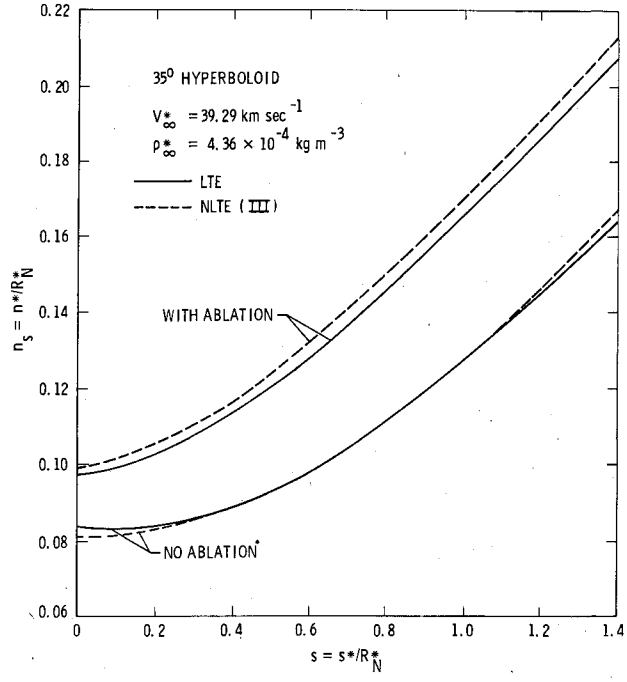

Fig. 6 Shock-standoff variation with distance along the body.

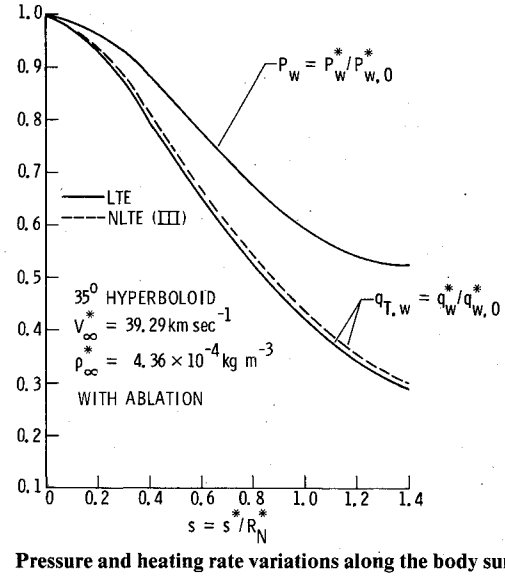

Fig. 7 Pressure and heating rate variations along the body surface.

The equilibrium and nonequilibrium shock-standoff variation with distance along the body surface is shown in Fig. 6 for cases with and without ablation injection. It is noted that the shock-standoff distance is not influenced significantly by the NLTE conditions for the case with no ablation injection. For the case with ablation injection, however, the NLTE (III) results are comparatively higher than the LTE results. The reason for this behavior is the combination of enthalpy and density variation in the shock layer along with the energy loss at the shock for nonequilibrium conditions. The difference in LTE and NLTE shock-layer density is relatively higher for the case with ablation than without ablation.[15] This density variation essentially results in higher shock-standoff distance for the case with ablation.

Variations in the nondimensional surface pressure and heating rate along the forebody of the probe are illustrated in Fig. 7. These quantities are nondimensionalized by their respective stagnation values of $p^*_{w,0}=6.309$ atm, $q^*_{w,0}$ (LTE) = 201.849 MW/m^2, and $q^*_{w,0}$ (NLTE) = 208.927 MW/m^2. It is seen that NLTE virtually has no influence on

Table 1 Wall radiative heat flux for the case with ablation under LTE and NLTE conditions

	Wall radiative heat flux q_R^*, MW/m^2				
$s=s^*/R_N^*$	q_R^*(LTE)	q_R^*(I)	q_R^*(II)	q_R^*(III)	q_R^*(IV)
0.0	201.849	206.774	209.017	208.927	211.987
0.2	188.172	193.127	196.020	195.891	201.497
0.4	164.709	169.658	173.278	173.127	178.165
0.6108	135.040	139.244	141.497	141.543	144.782
0.7854	110.900	114.765	115.900	115.974	120.841
1.200	75.012	78.767	80.256	79.012	80.572
1.500	58.271	61.813	61.570	61.902	62.090

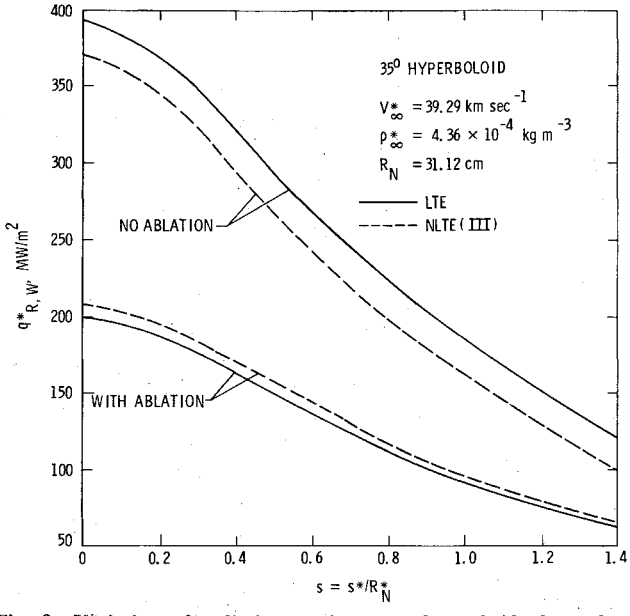

Fig. 8 Variation of radiative heating rate along the body surface (with and without ablation).

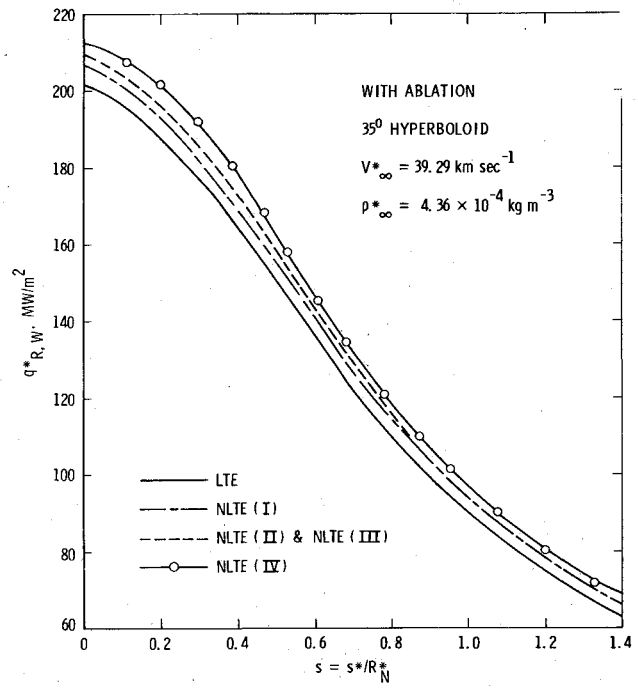

Fig. 9 Comparison of LTE and NLTE radiative heating rates along the body surface with ablation.

the pressure distribution. However, the total heating rate (convective plus radiative) is increased significantly under NLTE conditions. The main contribution to the total surface heating was found to be the radiative heating. The explanation of increased NLTE radiative heating, in this case, is given in the discussion of results presented in Figs. 8 and 9.

The results of radiative heating rates for different conditions are given in Table 1 and are shown in Figs. 8 and 9. The LTE and NLTE (III) results are compared in Fig. 8 for the cases with and without ablation injection. The results clearly indicate that the radiative heating to the body, in general, is reduced significantly in the presence of the ablative products. For the case with no ablation, the NLTE results are found to be significantly lower than the LTE results; a decrease of about 9% is noted at the stagnation point. Extensive discussion on this is presented in Refs. 11 and 15; but the main reason for this is that the NLTE source function is lower than the Planck function for identical conditions. In the presence of the ablative products, however, the results presented in Fig. 8 and Table 1 show the NLTE results are comparatively higher than the LTE results. The reason for this is as follows: Under NLTE conditions, the number of C_2 molecules in the ground state (that are capable of absorbing the incoming radiation from the shock-layer gases) is less as compared to the LTE values (i.e., the number based on the Boltzmann distribution). This increases the transparency of the ablation layer which, in turn, results in a higher heating rate of the entry body. This reverse trend in the NLTE heating rate is an important finding of this study. The results for the NLTE heating rate obtained by considering different radiative lifetimes are illustrated in Fig. 9. The results for cases η_r (II) and η_r (III) were found to be about the same for all body locations (see Table 1). The results for η_r (I) are seen to give the smallest increase in NLTE heating whereas the results for η_r (IV) provide the maximum heating rate to the body. These NLTE results, however, do not differ from each other considerably. The maximum increase in the stagnation-point heating is found to be about 3.5% for η_r (III) and about 5% for η_r (IV). Thus, based on the information of radiative lifetimes of the C_2-band system available at the present time, it may be concluded that the NLTE effects will be maximum for the combined radiative lifetime represented by η_r (IV), and this will increase the radiative heating of the body by a maximum of about 5%. This, in turn, would result in a relatively higher rate of mass loss from the body surface.[15]

VI. Conclusions

The radiative transfer equation has been formulated under the nonlocal thermodynamic equilibrium (NLTE) conditions. The formulation is used in solving the viscous radiating shock-layer equations with coupled ablation and mass injection for a Jovian entry probe with a carbon-phenolic heat shield. The Swan (0,0), Freymark (0,1), and Mulliken (0,0) bands of the C_2-band systems are treated to be in nonequilibrium in the ablation layer. Flowfield results obtained for the peak-heating conditions ($t=111.3$ s) indicate that the temperature distribution in the shock layer is lower under NLTE conditions. Similar behavior is also noticed for the enthalpy distribution. It is found that NLTE increases the density in the shock layer, but has no influence on the pressure variation. The radiative heating to the entry body is increased

significantly because of NLTE; this, in turn, results in increased mass loss from the body.

Acknowledgments

This work was supported by NASA Langley Research Center through Grant NSG-1500. The authors wish to express their thanks to Drs. Kenneth Sutton and J. N. Moss for several valuable discussions and suggestions.

References

[1] Page, W. A., "Aerodynamic Heating for Probe Vehicles Entering the Outer Planets," Paper AAS-71-144, American Astronautical Society, June 1971.

[2] Olstad, W. B., "Planetary Entry Aerothermodynamics," *Astronautics & Aeronautics*, Vol. 12, Nov. 1974, pp. 58-69.

[3] Walberg, G. D., Jones, J. J., Olstad, W. B., Sutton, K., Moss, J. N., and Powell, R. W., "Mass Loss Shape Change and Real-Gas Aerodynamic Effects on a Jovian Atmosphere Probe," *Acta Astronautica*, Vol. 4, May 1977, pp. 555-575.

[4] Nicolet, W. E., "Aerothermodynamic Environment for Jovian Entry Conditions," AIAA Paper 75-672, May 1975.

[5] Moss, J. N., Anderson, E. C., and Bolz, C. W., "Viscous-Shock-Layer Solutions with Radiation and Ablation Injections for Jovian Entry," AIAA Paper 75-671, 1975; also, *Progress in Astronautics and Aeronautics: Radiative Transfer and Thermal Control*, Vol. 49, edited by A. M. Smith, AIAA, New York, 1976, pp. 251-274.

[6] Moss, J. N., Anderson, E. C., and Bolz, C. W., "Aerothermal Environment for Jovian Entry Probes," AIAA Paper 76-469, 1976; also, *Progress in Astronautics and Aeronautics: Thermophysics of Spacecraft and Outer Planet Entry Probes*, Vol. 56, edited by A. M. Smith, AIAA, New York, 1977, pp. 333-354.

[7] Lincoln, K. A., Howe, J. T., and Liu, T. M., "Assessment of Chemical Nonequilibrium for Massively Ablating Graphite," *AIAA Journal*, Vol. 11, Aug. 1973, pp. 1198-1200.

[8] Sutton, K. and Moss, J. N., "Radiation Absorption by the C_2 Band Systems for the Jupiter Entry Conditions," AIAA Paper 79-0033, Jan. 1979.

[9] Moss, J. N., "A Study of the Aerothermal Entry Environment for the Galileo Probe," AIAA Paper 79-1081, 1979; also *Progress in Astronautics and Aeronautics: Entry Heating and Thermal Protection*, Vol. 69, edited by W. B. Olstad, AIAA, New York, 1980, pp. 3-25.

[10] Horton, T. E., "The Importance of Nonequilibrium in Estimating Radiating Heat Transfer Through a Flow," AIAA Paper 76-170, 1976; also, *Progress in Astronautics and Aeronautics: Thermophysics of Spacecraft and Outer Planet Entry Probes*, Vol. 56, edited by A. M. Smith, AIAA, New York, 1977, pp. 433-448.

[11] Tiwari, S. N. and Subramanian, S. V., "Nonequilibrium Radiative Heating of a Jovian Entry Body," AIAA Paper 79-0035, 1979; also, *Progress in Astronautics and Aeronautics: Entry Heating and Thermal Protection*, Vol. 69, edited by W. B. Olstad, AIAA, New York, 1980, pp. 83-103.

[12] Nelson, H. F., "Saturation Effects on Stagnation Radiative Heating for the Jupiter Probe," *AIAA Journal*, Vol. 18, Sept. 1980, pp. 1133-1140.

[13] Moss, J. N., "Reacting Viscous-Shock-Layer Solutions with Multicomponent Diffusion and Mass Injection," NASA TR-411, June 1974.

[14] Tiwari, S. N. and Szema, K. Y., "Effect of Precursor Heating on Radiating and Chemically Reacting Viscous Flow Around a Jovian Entry Body," NASA CR-3186, Oct. 1979; also *Progress in Astronautics and Aeronautics: Outer Planet Entry Heating and Thermal Protection*, Vol. 64, edited by R. Viskanta, AIAA, New York, 1979, pp. 129-146.

[15] Tiwari, S. N. and Subramanian, S. V., "Influence of Nonequilibrium Radiation and Shape Change on Aerothermal Environment of a Jovian Entry Body," NASA CR-3432, May 1981; also S. V. Subramanian, Ph.D. Dissertation, School of Engineering, Old Dominion University, Norfolk, Va., May 1980.

[16] Vincenti, W. A. and Kruger, C. H., *Introduction to Physical Gas Dynamics*, Wiley, New York, 1965.

[17] Jefferies, J. T., "Source Function in a Nonequilibrium Atmosphere: VII. The Interlocking Problem," *Astrophysical Journal*, Vol. 132, Nov. 1969, pp. 775-789; also, *Spectral Line Formation*, Blaisdell Publishing Co., Waltham, Mass., 1968.

[18] Kulander, J. L., "Curves of Growth for Nonequilibrium Gases," *Journal of Quantitative Spectroscopy and Radiative Transfer*, Vol. 8, June 1968, pp. 1319-1340.

[19] Tiwari, S. N. and Cess, R. D., "The Influence of Vibrational Nonequilibrium Upon Infrared Radiative Energy Transfer," *Journal of Quantitative Spectroscopy and Radiative Transfer*, Vol. 11, March 1971, pp. 237-248.

[20] Nicolet, W. E., "Advanced Methods for Calculating Radiation Transport in Ablation-Product Contaminated Boundary Layers," NASA CR-1656, Sept. 1970.

[21] McWhirter, R. W. P., "Spectral Intensities," *Plasma Diagnostic Techniques*, edited by R. H. Huddlestone and L. S. Leonard, Academic Press, New York, 1966.

[22] Cooper, D. M. and Nicholls, R. W., "Measurement of the Electronic Transition Moments of C_2 Band Systems," *Journal of Quantitative Spectroscopy and Radiative Transfer*, Vol. 15, Feb. 1975, pp. 139-150.

[23] Schadee, A., "The Relation Between the Electronic Oscillator Strength and the Wavelength for Diatomic Molecules," *Journal of Quantitative Spectroscopy and Radiative Transfer*, Vol. 7, Feb. 1967, pp. 169-183.